



Treatment of single and mixed pesticide formulations by solar photoelectro-Fenton using a flow plant

Fábio Gozzi^{a,b}, Ignasi Sirés^b, Abdoulaye Thiam^b, Silvio C. de Oliveira^a, Amílcar Machulek Junior^a, Enric Brillas^{b,*}

^a Instituto de Química (INQUI), Universidade Federal de Mato Grosso do Sul, Av. Senador Filinto Muller, 1555, CP 549, MS 79074-460 Campo Grande, Brazil

^b Laboratori d'Electroquímica dels Materials i del Medi Ambient, Departament de Química Física, Facultat de Química, Universitat de Barcelona, c/Martí i Franquès 1-11, 08028 Barcelona, Spain

HIGHLIGHTS

- Tebuthiuron and ametryn formulations degraded in a flow plant with BDD/air-diffusion cell.
- Growing oxidation power over single herbicide formulations: $AO-H_2O_2 < EF < SPEF$.
- Two-stage kinetics in EF and SPEF due to the formation of Fe(II) and Fe(III) complexes.
- Similar profiles with lower oxidation ability for mixed herbicide formulations in SPEF.
- Identification of 4 heteroaromatic products in mixtures and release of sulfate and nitrate ions.

ARTICLE INFO

Article history:

Available online xxx

Keywords:

Ametryn
Anodic oxidation
Electro-Fenton
Solar photoelectro-Fenton
Tebuthiuron
Water treatment

ABSTRACT

Solutions of single real formulations of herbicides tebuthiuron and ametryn have been degraded by anodic oxidation with electrogenerated H_2O_2 ($AO-H_2O_2$), electro-Fenton (EF) and solar photoelectro-Fenton (SPEF). The assays were made in a flow plant of 2.5 L equipped with a boron-doped diamond (BDD)/air-diffusion cell and a solar planar photoreactor. Main oxidants were hydroxyl radicals formed from water discharge at the BDD anode and in the bulk from Fenton's reaction between added Fe^{2+} and cathodically generated H_2O_2 . Partial mineralization was achieved for all the treatments, with the relative oxidation ability growing in the sequence: $AO-H_2O_2 < EF < SPEF$. The superiority of SPEF over EF was related to the contribution of photo-oxidation of intermediates and/or their Fe(III) complexes upon sunlight irradiation. No short-linear carboxylic acids were identified, whereas heteroatoms were mainly released as NO_3^- and SO_4^{2-} ions. For herbicide contents ≤ 0.18 mM in EF and SPEF, a very rapid pseudo-first-order decay kinetics was related to the oxidation of the Fe(II) complexes of each herbicide at short time, whereupon a much slower pseudo-first-order kinetics associated with the decay of their Fe(III) complexes was observed. Ametryn disappeared more quickly than tebuthiuron, but its solutions were more poorly mineralized. The effect of j and substrate concentration on the performance of SPEF was examined. Mixtures of both formulations were efficiently treated by SPEF, showing similar but slower decays than single solutions. Four primary heteroaromatic products were detected by GC–MS upon prolonged electrolysis of an equimolar mixture. Our results indicate that SPEF is viable for the treatment of water contaminated with tebuthiuron and ametryn herbicides, either single or mixed.

© 2016 Elsevier B.V. All rights reserved.

1. Introduction

The high consumption of commercial pesticides in agriculture as well as the inadequate disposal or storage of obsolete products lead to the accumulation of herbicides in soil, air and water. Since

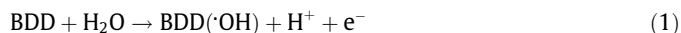
this pollution exerts toxic effects on living beings, agricultural wastewater needs to be treated before being released into the aquatic environment [1]. In some cases, high concentrations of up to 500 mg L^{-1} of herbicides have been detected in such wastewater [1]. Commercial formulations of the urea herbicide tebuthiuron ($C_9H_{16}N_4OS$, 1-(5-*tert*-butyl-1,3,4-thiadiazol-2-yl)-1,3-dimethylurea) and the s-triazine herbicide ametryn ($C_9H_{17}N_5S$, 2-ethylamino-4-isopropylamino-6-methylthio-s-triazine) are widely employed in Brazil to control sugar cane cultivations [2]. These

* Corresponding author. Tel.: +34 934021223; fax: +34 934021231.

E-mail addresses: machulekjr@gmail.com (A.M. Junior), brillas@ub.edu (E. Brillas).

substances have been detected in soil treated with sugar cane vinasse [3] and natural water and wastewater [4,5], because of their high solubility in water and inefficient destruction in wastewater treatment plants. Several works have described the destruction of tebuthiuron solutions by advanced oxidation processes (AOPs) like TiO_2 photocatalysis [6,7] and photo-Fenton [8,9], based on the in situ generation of $\cdot\text{OH}$. The high standard reduction potential of this strong oxidant ($E^\circ(\cdot\text{OH}/\text{H}_2\text{O}) = 2.8 \text{ V/SHE}$ [10]) favors its reaction with most organics, eventually leading to their total mineralization. Regarding ametryn, its removal from aqueous solutions has been achieved by Cl_2 [11], $\text{UV}/\text{H}_2\text{O}_2$ [12] and visible light with porphyrins as sensitizers [13], whereas commercial mixtures have been treated by solar TiO_2 photocatalysis [14]. However, less is known about the performance of electrochemical AOPs (EAOPs). Alves et al. [15] electrolyzed 400 mL of a 100 mg L^{-1} tebuthiuron solution in a stirred tank reactor with a boron-doped diamond (BDD) anode and a Pt cathode at current densities (j) of $10\text{--}200 \text{ mA cm}^{-2}$, finding that the herbicide decayed following a pseudo-first-order kinetics with a maximum apparent rate constant of 0.32 min^{-1} and a maximum mineralization of 80% at 200 mA cm^{-2} , with loss of nitrate ion.

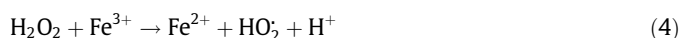
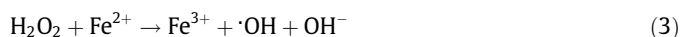
Recently, EAOPs such as anodic oxidation (AO), electro-Fenton (EF) and photoelectro-Fenton (PEF) have received increasing attention for the degradation of recalcitrant and/or toxic organics in water [10,16–18]. AO is the most widespread process and consists in the application of a high j to directly oxidize the pollutants at the surface of the anode M and, to a larger extent, under the action of physisorbed hydroxyl radicals $\text{M}(\cdot\text{OH})$ formed from the anodic oxidation of water [16]. Currently, the preferred anodes for AO are the BDD thin-film electrodes, which possess higher oxidation power than other common anodes like Pt and PbO_2 [19–23] as a result of their larger O_2 -overpotential and the very low interaction between their surface and $\cdot\text{OH}$, thus favoring the reaction of $\text{BDD}(\cdot\text{OH})$ with organics. This radical is produced as follows [16,24–26]:



The combination of AO with a cathode able to generate H_2O_2 in an undivided cell gives rise to the so-called AO with electrogenerated H_2O_2 (AO- H_2O_2) process [17]. This treatment involves the destruction of organics by physisorbed $\text{M}(\cdot\text{OH})$, along with the minor contribution of other reactive oxygen species (ROS) like H_2O_2 and its anodic oxidation product HO_2 [10,17]. H_2O_2 can be efficiently produced via the two-electron reduction of O_2 gas via reaction (2) at carbonaceous cathodes such as metal-modified carbon [27], activated carbon fiber [28], carbon nanotubes [29], graphite felt [30], carbon felt [31–33], carbon-polytetrafluoroethylene (PTFE) O_2 or air-diffusion [34–36] and BDD [37].

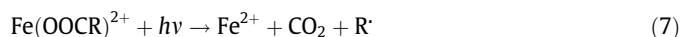


The oxidation ability of H_2O_2 generated in a cell used for AO- H_2O_2 with a BDD anode can be strongly improved by EF upon addition of a small quantity of Fe^{2+} ion to the solution to promote the Fenton's reaction (3) [30–37], which is catalytic and can be propagated from Fe^{2+} regeneration by Fenton-like reaction (4) and cathodic Fe^{3+} reduction reaction (5).



The EF process operates at optimum pH near 3 with destruction of organics by two main kinds of ROS, $\text{M}(\cdot\text{OH})$ at the anode surface and $\cdot\text{OH}$ in the bulk [38,39]. In our laboratory, we are also develop-

ing the PEF process with UVA light [40] and the solar PEF (SPEF) [40–43] as more powerful alternatives than EF for wastewater treatment. In PEF or SPEF, the solution is simultaneously irradiated with either artificial UVA light or sunlight, respectively. We found that SPEF becomes much more efficient and cost-effective due to the use of free and renewable sunlight that supplies a higher UV intensity compared to UVA lamps. This radiation can produce two main phenomena: (i) the photoreduction of $\text{Fe}(\text{OH})^{2+}$ species, which predominates at pH ~ 3 , to Fe^{2+} with $\cdot\text{OH}$ generation via reaction (6), and (ii) the photodecomposition of complexes of Fe (III) with intermediates from aromatics or heteroaromatics degradation, like carboxylic acids by reaction (7).



To gain a better knowledge about the possible viability of SPEF for the treatment of agricultural wastewater at industrial scale, this paper presents the degradation of commercial formulations of tebuthiuron and ametryn, either single or mixed, by this method at pH 3.0 using a flow plant of 2.5 L equipped with a BDD/air-diffusion cell coupled with a solar planar reactor. The effect of j and herbicide concentration on the performance of SPEF was examined. Comparable AO- H_2O_2 and EF assays were carried out as well to better clarify the role of generated hydroxyl radicals and sunlight. The decay of each herbicide was followed by high-performance liquid chromatography (HPLC), whereas primary heteroaromatics formed from mixed equimolar formulation solutions were identified by gas chromatography–mass spectrometry (GC–MS). Released inorganic ions were detected by ion chromatography.

2. Materials and methods

2.1. Chemicals

Commercial formulations of Combine 500 SC® with 500 g L^{-1} of tebuthiuron and Gesapax® with 500 g L^{-1} ametryn were purchased from Syngenta and used as received. Analytical grade tebuthiuron (>99% purity) and ametryn (>99% purity) from Sigma–Aldrich were used as standards. Anhydrous sodium sulfate and heptahydrated Fe(II) sulfate were of analytical grade from Merck and Fluka, respectively. Deionized water was used to prepare the solutions and their pH was adjusted to 3.0 with analytical grade sulfuric acid from Merck. Other chemicals for analyses were either of HPLC or analytical grade supplied by Sigma–Aldrich, Merck and Panreac.

2.2. Solar flow plant

The batch recirculation flow plant used to degrade 2.5 L of solutions with single herbicide formulations and their mixtures has been described elsewhere [41]. The main components of the plant were: (i) a reservoir to contain the solution, (ii) a centrifugal pump for its recirculation, (iii) a flowmeter to keep the liquid flow rate at 200 L h^{-1} , (iv) two heat exchangers to maintain the solution temperature at 35°C , (v) a filter-press electrochemical cell and (vi) a planar solar photoreactor for the SPEF trials. The electrochemical cell contained a 20 cm^2 BDD anode from NeoCoat and a 20 cm^2 carbon-PTFE air-diffusion cathode from E-TEK, with an interelectrode gap of 1.2 cm. The inner face of the cathode was in contact with a gas chamber where an air flow at an overpressure of about 8.6 kPa regulated with a back-pressure gauge was continuously injected for H_2O_2 production. An Agilent 6552A DC power supply was used to apply a constant j to the cell, as well as to monitor the potential difference between the anode and cathode. The solar planar photoreactor with 600 mL of irradiated volume was tilted

41° (latitude of our laboratory in Barcelona) to better collect the direct sun rays. Comparative AO-H₂O₂ and EF trials were performed in the dark by covering the plant with an opaque plastic. SPEF assays were made in clear and sunny days during the summer of 2015 and the UV radiation intensity (300–400 nm) supplied by sunlight was about 30–32 W m⁻², as determined with a Kipp&Zonen CUV 5 radiometer.

2.3. Instruments and analytical procedures

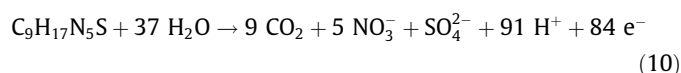
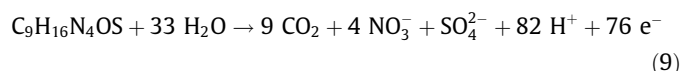
The solution pH was determined with a Crison 2000 pH-meter. The kinetic decay of herbicides was assessed by reversed-phase HPLC upon injection of 20 µL aliquots into a Waters 600 LC fitted with a Waters Spherisorb ODS2-C18 5 µm, 150 mm × 4.6 mm, column at 40 °C and coupled to a Waters 996 photodiode array detector set at 249 nm for tebuthiuron and 222 nm for ametryn. All the samples withdrawn from treated solutions were filtered with Whatman 0.45 µm PTFE filters and, furthermore, for the kinetic analysis in EF and PEF, they were previously diluted (1:1) with acetonitrile to stop the degradation process. The mobile phases were a 25:75 (v/v) acetonitrile/water mixture at 0.6 mL min⁻¹ for analyzing tebuthiuron alone, a 60:40 (v/v) acetonitrile/water mixture at 0.8 mL min⁻¹ for analyzing ametryn alone and a 40:60 (v/v) acetonitrile/water (1 mM ammonium acetate) mixture at 0.8 mL min⁻¹ when both formulations were mixed.

Analysis of short-linear aliphatic carboxylic acids was made by ion-exclusion HPLC with the same LC system fitted with a Bio-Rad Aminex HPX 87H, 300 mm × 7.8 mm, column at 35 °C and the photodiode detector selected at λ = 210 nm. To do this, 20 µL aliquots were injected into the LC and a 4 mM H₂SO₄ solution was eluted at 0.6 mL min⁻¹ as mobile phase. NH₄⁺, NO₃⁻ and SO₄²⁻ ions were identified and quantified as previously reported [34,35,43] from the degradation of 100 mL of formulation solutions with 0.05 M LiClO₄, adjusted to pH 3.0 with HClO₄ to avoid the interference of ions of sulfate medium, using a stirred BDD/air-diffusion tank reactor at 35 °C.

For the mineralization experiments, the samples withdrawn from treated solutions at regular times were filtered with Whatman 0.45 µm PTFE filters, and their total organic carbon (TOC) content was determined immediately on a Shimadzu VCSN TOC analyzer. Reproducible TOC values with ±1% accuracy were found by injecting 50 µL aliquots into the above analyzer. These data were then utilized to estimate the mineralization current efficiency (MCE) for each electrolysis at current *I* (in A) and time *t* (in min) from Eq. (8) [42]:

$$\text{MCE (\%)} = \frac{n F V \Delta(\text{TOC})_{\text{exp}}}{4.32 \times 10^7 m I t} \times 100 \quad (8)$$

where *F* is the Faraday constant (96,487 C mol⁻¹), *V* is the solution volume (in L), Δ(TOC)_{exp} is the experimental TOC decay (in mg C L⁻¹), 4.32 × 10⁷ is a conversion factor (3600 s h⁻¹ × 12,000 mg C mol⁻¹) and *m* is the number of carbon atoms of the herbicide (9 C atoms for each compound). The number of electrons *n* involved in the mineralization process was taken as 76 for tebuthiuron and 84 for ametryn, according to reactions (9) and (10), respectively, considering their total conversion into CO₂, nitrate and sulfate, as will be discussed below.



For mixed herbicide formulations, the average number of electrons *n* for total mineralization was calculated as: 76 *x*_{tebuthiuron} + 84 *x*_{ametryn}, where *x_i* is the molar fraction of the herbicide *i*.

The specific energy consumption per unit TOC mass removed (EC_{TOC}) at a given time *t* (in h) of each trial was determined as follows [41]:

$$\text{EC}_{\text{TOC}} (\text{kWh g}^{-1} \text{TOC}) = \frac{E_{\text{cell}} I t}{V \Delta(\text{TOC})_{\text{exp}}} \quad (11)$$

where *E_{cell}* is the average potential difference between electrodes.

The primary heteroaromatic products formed during the SPEF treatment of 2.5 L of a mixed equimolar solution of tebuthiuron and ametryn formulations at 50 mA cm⁻² for 180 min were analyzed by GC–MS. The organic components of 5 × 100 mL of the remaining solution were extracted each one with 25 mL of CH₂Cl₂. The resulting organic fractions were mixed up, dried over anhydrous Na₂SO₄, filtered and rotavaporated up to ca. 1 mL. GC–MS analysis of this sample as well as of raw formulations was made with an Agilent Technologies system composed of a 6890N GC, fitted with a non-polar Teknokroma Sapiens-X5ms 0.25 µm, 30 m × 0.25 mm, column, and a 5975C MS operating in EI mode at 70 eV. The temperature ramp was: 36 °C for 1 min, 5 °C min⁻¹ up to 320 °C and hold time 10 min. The temperature of the inlet, source and transfer line was 250, 230 and 300 °C. The mass spectra were identified using a NIST05-MS library.

3. Results and discussion

3.1. Degradation of single tebuthiuron formulations by AO-H₂O₂, EF and SPEF

First assays were performed with 2.5 L of a solution with 20 mg L⁻¹ TOC of tebuthiuron formulation in 0.05 M Na₂SO₄ at pH 3.0. A reversed-phase chromatogram of this solution displayed a well defined peak accounting for 0.18 mM herbicide, as determined from a calibration curve with a pure standard. From this herbicide content, it was concluded that the commercial formulation contained tebuthiuron as the sole organic compound. The above solution was recirculated at 200 L h⁻¹ through the flow plant under sunlight irradiation and without applied current and no change in herbicide content was observed for 240 min, indicating that the substrate was not photosensitive. The same behavior was found upon addition of 0.50 mM Fe²⁺. In contrast, the solution with 0.50 mM Fe³⁺ (in the form of hydrated sulfate) was photosensitive, since herbicide decay was ~40% after 420 min of sunlight exposure. This suggests the formation of photolizable Fe(III)-tebuthiuron complexes, as expected from the affinity of the thiadiazole ring of the herbicide with iron ions [9]. In addition, some contribution from ·OH induced by photolytic reaction (6) could be expected as well. One can then expect that, in the presence of Fe²⁺, Fe(II)-tebuthiuron complexes are also produced, although they do not undergo photodecomposition.

Fig. 1a depicts the decay of the normalized herbicide concentration of the above solution upon treatment by AO-H₂O₂, EF and SPEF at 50 mA cm⁻². A slow but continuous removal of tebuthiuron can be observed in the former treatment, only attaining 74% abatement after 360 min of electrolysis. This is indicative of a very slow attack of BDD(·OH) formed from reaction (1) onto the substrate. On the other hand, Fig. 1a shows a more complex concentration decay during the EF and SPEF assays. In both cases, about 50% of herbicide removal was reached in only 3 min, whereupon it dropped very slowly to disappear in 300 and 240 min, respectively. The very fast removal of tebuthiuron at the beginning of EF and SPEF can be explained by the rapid destruction of the raw herbicide and/or its Fe(II) complexes by ·OH originated from Fenton's reaction (3), whereas the significant deceleration at longer time can be associated with the abatement of its Fe(III) complexes. It is well known that Fe³⁺ is rapidly accumulated in solution when the EF and SPEF

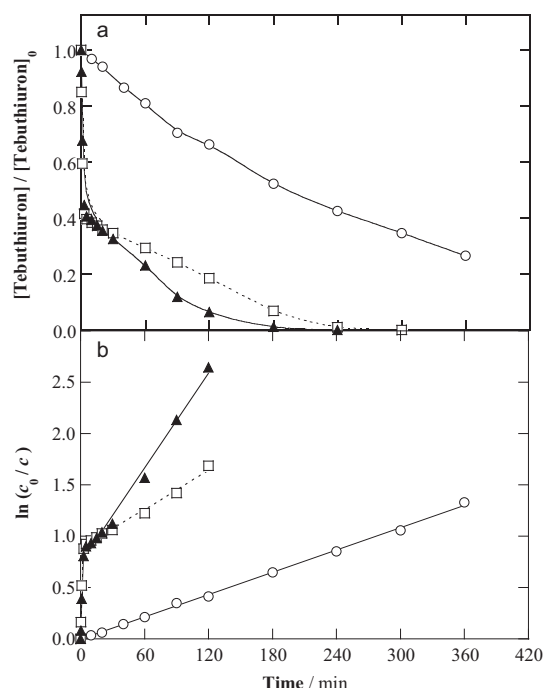


Fig. 1. (a) Normalized tebuthiuron concentration vs. electrolysis time and (b) the corresponding kinetic analysis assuming a pseudo-first-order reaction for the degradation of 2.5 L of solutions with herbicide formulation of 20 mg L^{-1} TOC in $0.05 \text{ M Na}_2\text{SO}_4$ at pH 3.0 and 35°C using a flow plant with a BDD/air-diffusion cell of 20 cm^2 electrode area coupled with a solar photoreactor of 600 mL irradiation volume at j of 50 mA cm^{-2} and liquid flow rate of 200 L h^{-1} . Method: (○) anodic oxidation with electrogenerated H_2O_2 (AO- H_2O_2), (□) electro-Fenton (EF) with 0.50 mM Fe^{2+} and (▲) solar photoelectro-Fenton (SPEF) with 0.50 mM Fe^{2+} .

processes are performed with a gas-diffusion cathode because its large efficiency for H_2O_2 production hinders the regeneration of Fe^{2+} from Fe^{3+} reduction by reaction (5) [10,17]. In EF, the large amounts of $\text{Fe(III)-tebuthiuron}$ complexes formed are removed by the attack of both, $\text{BDD}(\cdot\text{OH})$ and the quantities of $\cdot\text{OH}$ produced by the remaining Fe^{2+} . The quicker herbicide decay in SPEF (see Fig. 1a) can then be due to the combination of additional $\cdot\text{OH}$ induced from photolytic reaction (6) and the photolysis of $\text{Fe(III)-tebuthiuron}$ complexes, as pointed out above.

The above concentration decays were analyzed by kinetic equations related to simple reaction orders. Fig. 1b presents the good linear correlation obtained for a pseudo-first-order reaction during all the AO- H_2O_2 treatment, which can be ascribed to the attack of a constant amount of $\text{BDD}(\cdot\text{OH})$ onto the herbicide. In contrast, the kinetic decays for EF and SPEF can be described by two consecutive linear profiles, also related to pseudo-first-order reactions. This agrees with the rapid oxidation of the substrate and/or its Fe(II) complexes with a constant amount of $\cdot\text{OH}$ at short times, followed by a much slower destruction of $\text{Fe(III)-tebuthiuron}$ species by smaller constant quantities of that homogeneous radical and heterogeneous $\text{BDD}(\cdot\text{OH})$, as stated above. The corresponding pseudo-first-order rate constants (k_1) found from such kinetic analysis are summarized in Table 1. The EF and SPEF processes presented similar k_1 values at short time, as expected if $\cdot\text{OH}$ in the bulk is the main oxidant of the herbicide and/or its Fe(II) species. The k_1 values at longer time were 44 and 18 times lower, respectively, because of the slow oxidation of its Fe(III) complexes by both, $\text{BDD}(\cdot\text{OH})$ and the smaller amounts of $\cdot\text{OH}$. The greater k_1 value for SPEF is then due to the photolytic action of sunlight, as pointed out above. The AO- H_2O_2 process yielded a k_1 value about 2-fold lower than that of EF at long time, corroborating the oxidation by $\cdot\text{OH}$ in Fenton systems.

The TOC-time plots determined for the above trials are depicted in Fig. 2a. In all these assays, no significant change in solution pH was found. Partial mineralization of 36%, 53% and 70% was obtained after 360 min of AO- H_2O_2 , EF and SPEF, respectively (see Table 1), meaning that the oxidation ability of these EAOPs increased in the order: AO- H_2O_2 < EF < SPEF. The lowest oxidation power of AO- H_2O_2 can be ascribed to the slow destruction of intermediates by $\text{BDD}(\cdot\text{OH})$ [16], which is accelerated in EF and SPEF by their parallel oxidation by $\cdot\text{OH}$. It should be noted that no carboxylic acids were detected in none of these treatments by ion-exclusion HPLC. This points to consider that the superiority of SPEF is mainly due to the photolysis of other oxidation products and/or their Fe(III) complexes [17,38].

In order to determine the inorganic ions released during the above EAOPs, 100 mL of a 0.46 mM tebuthiuron solution in 0.05 M LiClO_4 with 0.50 mM Fe^{2+} of pH 3.0 were degraded under EF conditions using a stirred BDD/air-diffusion cell of 3 cm^2 electrode area. After 360 min at $j = 100 \text{ mA cm}^{-2}$, 0.52 mM of NO_3^- ion (28.2% of initial N) and 0.46 mM of SO_4^{2-} ion (100% of initial S) were detected in the treated solution by ion chromatography, whereas no NH_4^+ ion was found. These results indicate that the initial N atoms were mainly lost in the form of volatile species such as N_2 and N_xO_y [40–43], confirming the overall mineralization reaction (9) for tebuthiuron.

Based on the above finding, the MCE values for the data of Fig. 2a were calculated from Eq. (8) and the results obtained are presented in Fig. 2b. As expected, higher current efficiency was found when increasing the oxidation ability of EAOPs, being SPEF the most efficient process (see also Table 1). Note that the MCE value remained practically constant in each treatment, at least for times longer than 120 min. This behavior suggests a quite constant mineralization rate of the intermediates under the action of hydroxyl radicals and/or sunlight.

The EC_{TOC} values for the same experiments are presented in Fig. 2c. They dropped as the current efficiency of the EAOPs increased, presenting an almost constant value for each treatment. SPEF was then the most inexpensive process, with a specific energy consumption of $2.23 \text{ kWh g}^{-1} \text{ TOC}$ (39.1 kWh m^{-3}) at 360 min (see Table 1).

The influence of j on the mineralization rate in the EF and SPEF processes was further examined since this parameter regulates the amount of oxidizing hydroxyl radicals formed. As an example, Fig. 3a depicts the TOC-time curves obtained by SPEF between 25 and 100 mA cm^{-2} . A gradual acceleration of TOC decay can be observed with raising j , as expected by the concomitant increase in rate of reaction (1), producing greater amounts of $\text{BDD}(\cdot\text{OH})$, and of reaction (2) yielding greater quantity of H_2O_2 that enhances $\cdot\text{OH}$ production. The quicker oxidation of intermediates favors the generation of species that are more rapidly photolyzed, enhancing the decontamination in SPEF. A higher mineralization removal at greater j was also found for EF (see Table 1), always being lower than that in SPEF. Fig. 3b highlights the opposite trend for MCE, which dropped with raising j , whereas Fig. 3c evidences the corresponding growth of EC_{TOC} due to the concomitant rise in E_{cell} . This behavior was accomplished for both EF and SPEF (see Table 1). For the latter process, the best final values in terms of energy were 20.3% of current efficiency with an energy consumption of $0.93 \text{ kWh g}^{-1} \text{ TOC}$ (12.0 kWh m^{-3}) at 25 mA cm^{-2} , but with only 53% mineralization.

The decay in MCE as j increases is accomplished for all EAOPs [10,16,17], being a phenomenon that can be explained by the acceleration of parasitic non-oxidizing reactions of hydroxyl radicals, which causes a decrease of their relative concentration with the consequent reduction of reactive events with organic molecules. Examples of such parasitic reactions are the anodic oxidation of physisorbed $\text{BDD}(\cdot\text{OH})$ to O_2 via reaction (12) and the removal of

Table 1

Pseudo-first-order rate constants and percentage of TOC removal, mineralization current efficiency and specific energy consumption per unit TOC mass removed after 360 min of the degradation of 2.5 L of solutions containing tebuthiuron and/or ametryn in 0.05 M Na₂SO₄ of pH 3.0 in a solar flow plant at liquid flow rate of 200 L h⁻¹ for different treatments at selected experimental conditions.

Method	[Tebuthiuron] (mM)	[Ametryn] (mM)	j^b (mA cm ⁻²)	k_1 (min ⁻¹)	R^2	% TOC removal	% MCE	EC _{TOC} (kWh g ⁻¹ TOC)
AO-H ₂ O ₂	0.18	–	50	3.6×10^{-3}	0.998	36	6.5	4.36
	–	0.18	50	1.4×10^{-2}	0.995	24	4.7	6.71
EF ^a	0.18	–	25	– ^c	– ^c	42	15.0	1.00
	0.18	–	50	0.28 ^d	0.980 ^d	53	9.2	2.71
				6.3×10^{-3e}	0.991 ^e			
	0.18	–	100	– ^c	– ^c	62	5.4	6.40
	–	0.18	25	– ^c	– ^c	43	17.0	1.04
	–	0.18	50	0.29 ^f	0.981 ^f	47	9.0	3.28
				2.6×10^{-2g}	0.999 ^g			
	–	0.18	100	– ^c	– ^c	52	5.2	7.87
	0.04	–	50	0.56 ^d	0.980 ^d	55	2.6	10.71
				4.2×10^{-2e}	0.998 ^e			
SPEF ^a	0.18	–	25	– ^c	– ^c	53	20.3	0.93
	0.18	–	50	0.27 ^d	0.983 ^d	70	11.2	2.23
				1.5×10^{-2e}	0.991 ^e			
	0.18	–	100	– ^c	– ^c	75	6.7	6.40
	1.80	–	50	7.0×10^{-3}	0.985	41	68.8	0.41
	–	0.04	50	0.62 ^f	0.979 ^f	35	1.9	16.70
				6.5×10^{-2g}	0.990 ^g			
	–	0.18	25	– ^c	– ^c	51	21.0	0.86
	–	0.18	50	0.30 ^f	0.979 ^f	52	11.2	2.61
				3.3×10^{-2g}	0.994 ^g			
	–	0.18	100	– ^c	– ^c	58	6.1	4.51
	–	0.72	50	1.0×10^{-2}	0.991	42	32.0	1.03
	0.18	0.09	50	9.8×10^{-2d}	0.988 ^d	53	14.9	2.08
				9.4×10^{-3e}	0.988 ^e			
				0.26 ^f	0.981 ^f			
				2.7×10^{-2g}	0.994 ^g			
	0.18	0.18	50	3.2×10^{-2d}	0.978 ^d	51	20.9	1.51
				8.1×10^{-3e}	0.985 ^e			
				0.19 ^f	0.980 ^f			
				2.7×10^{-2g}	0.991 ^g			
	0.18	0.36	50	– ^c	– ^c	48	25.6	1.25

^a With addition of 0.50 mM Fe²⁺.

^b Applied current density.

^c Not determined.

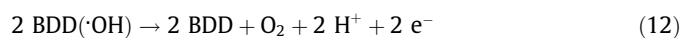
^d Data for tebuthiuron at short time.

^e Data for tebuthiuron at long time.

^f Data for ametryn at short time.

^g Data for ametryn at long time.

·OH by H₂O₂ and Fe²⁺ via reactions (13) and (14), respectively [10,17]. Moreover, the H₂O discharge from reaction (1) can be hampered by the larger formation of other weaker oxidants at the BDD anode like ozone via reaction (15) and S₂O₈²⁻ from SO₄²⁻ of the electrolyte via reaction (16) [16,17].



Another important operation parameter is the substrate concentration since it determines the oxidation ability of hydroxyl radicals and/or the photo-oxidation by sunlight. The effect of this parameter in SPEF was examined for 5, 20 and 200 mg L⁻¹ TOC of tebuthiuron formulation, corresponding to 0.04, 0.18 and 1.80 mM of the herbicide, at 50 mA cm⁻². Fig. 4a shows that complete removal required longer time with raising substrate concentration, as expected by the slower reaction of greater organic load with similar amounts of generated hydroxyl radicals. Interestingly, the rapid concentration abatement during the first stage falls

strongly as herbicide content increases. Thus, after 3 min of treatment, tebuthiuron was reduced by 82% at 0.04 mM, but only by 18% at 1.80 mM. This phenomenon suggests that, at lower herbicide contents, a larger proportion of the substrate is in the form of Fe(II)–tebuthiuron complexes, still remaining in solution enough Fe²⁺ to produce ·OH from Fenton's reaction, whereas at higher contents most of the Fe²⁺ is complexed. This is also reflected in the inset panel of Fig. 4a, since two consecutive pseudo-first-order kinetics can be represented for 0.04 and 0.18 mM, in agreement with the consecutive formation of Fe(II) and Fe(III) complexes, but only one linear correlation was observed for 1.80 mM, where Fe(III)–tebuthiuron species are slowly oxidized. Table 1 highlights that the k_1 values at short and long times decreased with increasing substrate content. The normalized TOC removal of Fig. 4b also evidences the existence of a slower mineralization at higher herbicide concentration, except at times >240 min in which the degradation of the 0.04 mM solution is decelerated by the generation of very recalcitrant products. However, higher MCE and lower EC_{TOC} values were determined at greater organic load (see Table 1). The most efficient process was found for the highest 1.80 mM concentration, with 41% TOC reduction, 68.8% of current efficiency and 0.41 kWh g⁻¹ TOC (36.5 kWh m⁻³) at 360 min. This trend suggests the availability of more amounts of BDD(·OH) and ·OH to destroy higher quantities of intermediates in detriment of their consumption by parasitic reactions (12)–(14).

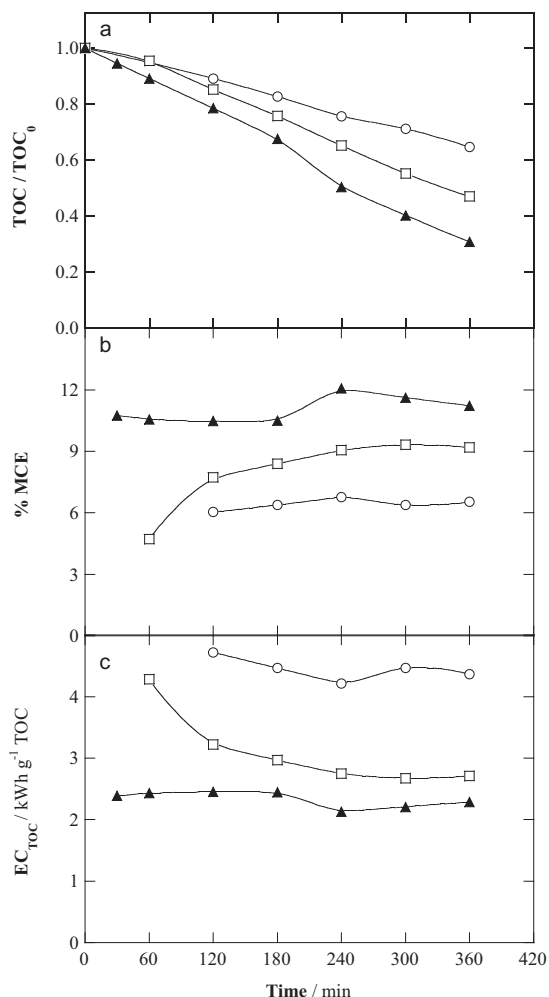


Fig. 2. (a) Normalized TOC removal, (b) mineralization current efficiency and (c) specific energy consumption per unit TOC mass removed for the trials given in Fig. 1. Method: (○) AO-H₂O₂, (□) EF with 0.50 mM Fe²⁺ and (▲) SPEF with 0.50 mM Fe²⁺.

3.2. Treatment of single ametryn formulations by AO-H₂O₂, EF and SPEF

A comparative study on the degradation of ametryn formulations was also performed in the same flow plant to assess the decontamination trends compared to those of tebuthiuron. Overall, a quite similar behavior was observed for both herbicides in the different EAOPs. Thus, it was found that the ametryn formulation uniquely contained the herbicide as organic matter, agreeing its concentration determined by standards with analyzed solution TOC. Its concentration decay also showed two consecutive pseudo-first-order kinetics, but no significant photolysis of complexes of Fe(II) or Fe(III) with ametryn was observed, which also allows discarding a significant contribution of $\cdot\text{OH}$ from reaction (6). The pH of its solutions did not vary significantly during the trials, no carboxylic acids were detected in treated solutions and the initial N and S atoms were partially and completely converted into NO_3^- and SO_4^{2-} ions, respectively, as stated in the total mineralization reaction (10) for ametryn. The most relevant results obtained are summarized in Table 1.

For a 20 mg L⁻¹ TOC solution, which corresponds to 0.18 mM ametryn, Fig. 5 shows that, operating at 50 mA cm⁻², it dropped very slowly in AO-H₂O₂, due to its slow reaction with BDD($\cdot\text{OH}$), disappearing after 360 min. In contrast, the most effective attack

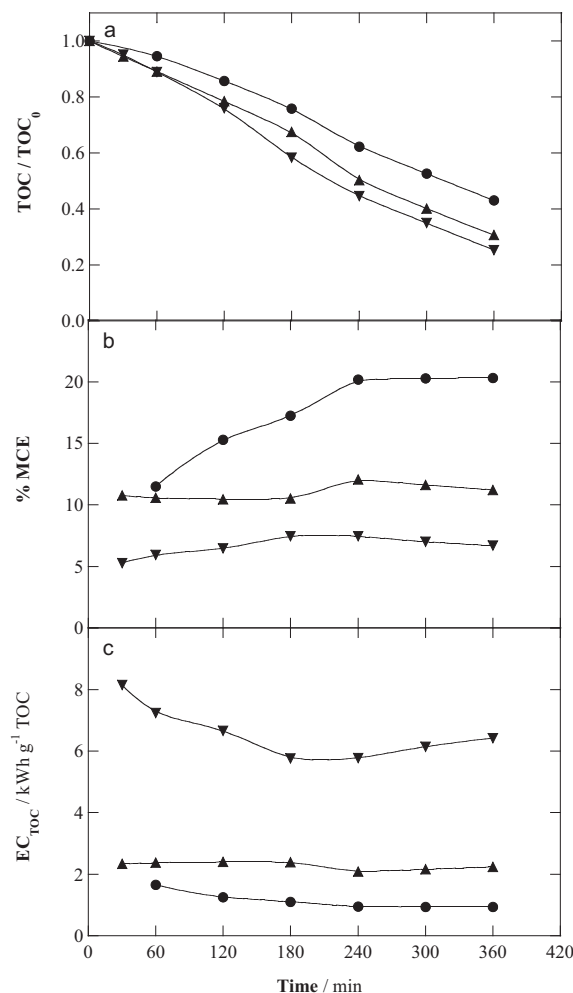


Fig. 3. Effect of current density on the change of (a) normalized TOC, (b) mineralization current efficiency and (c) specific energy consumption per unit TOC mass removed with electrolysis time for the SPEF treatment of 2.5 L of solutions with the tebuthiuron formulation of 20 mg L⁻¹ TOC in 0.05 M Na₂SO₄ with 0.50 mM Fe²⁺ at pH 3.0 and 35 °C using a solar flow plant at liquid flow rate of 200 L h⁻¹. Applied j : (●) 25 mA cm⁻², (▲) 50 mA cm⁻² and (▼) 100 mA cm⁻².

of additional $\cdot\text{OH}$ in EF and SPEF caused an analogous and faster removal with total abatement in about 120 and 90 min, respectively. The inset panel of Fig. 5a highlights the good pseudo-first-order kinetics found upon AO-H₂O₂ conditions and the two excellent consecutive straight lines determined in EF and SPEF. For the two latter processes, Table 1 shows similar k_1 values at short time, further decreasing near 11 and 9 times at long time, respectively, but still being 2-fold higher than the k_1 value for AO-H₂O₂. These findings demonstrate the role of $\cdot\text{OH}$ to cause: (i) a fast removal of the Fe(II) complexes of the substrate at short time, yielding high k_1 values, and (ii) a slower removal of its Fe(III) complexes at long time, giving rise to a strong k_1 reduction. In both cases, the $\cdot\text{OH}$ acts in concomitance with BDD($\cdot\text{OH}$), whose contribution is less significant according to the lower k_1 data found for AO-H₂O₂. The fact that the concentration decays always obeyed a pseudo-first-order kinetics suggests a constant production of BDD($\cdot\text{OH}$), large contents of $\cdot\text{OH}$ at short time and small contents of $\cdot\text{OH}$ at long time, as pointed out above. The slightly higher k_1 value at long time for SPEF than EF can be ascribed to additional production of $\cdot\text{OH}$ from reaction (6). Based on comparison of Figs. 1 and 5, it is evident that ametryn is more rapidly removed than tebuthiuron in all the EAOPs, as also deduced from k_1 values (Table 1).

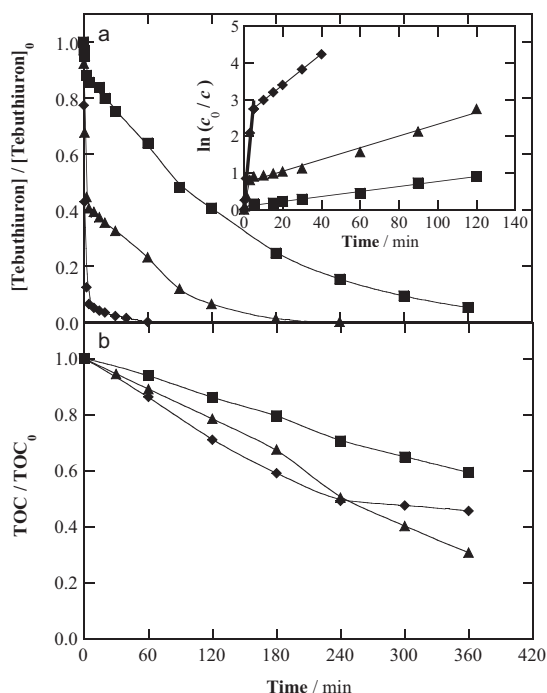


Fig. 4. (a) Effect of formulation content on the normalized abatement of tebuthiuron with electrolysis time for the SPEF degradation of 2.5 L of solutions in 0.05 M Na₂SO₄ and 0.50 mM Fe²⁺ at pH 3.0 and 35 °C in a solar flow plant at 50 mA cm⁻² and liquid flow rate of 200 L h⁻¹. TOC (herbicide) content: (◆) 5 mg L⁻¹ (0.04 mM), (▲) 20 mg L⁻¹ (0.18 mM) and (■) 200 mg L⁻¹ (1.80 mM). The inset panel shows the kinetic analysis considering a pseudo-first-order reaction. (b) Time-course of normalized TOC for the same assays.

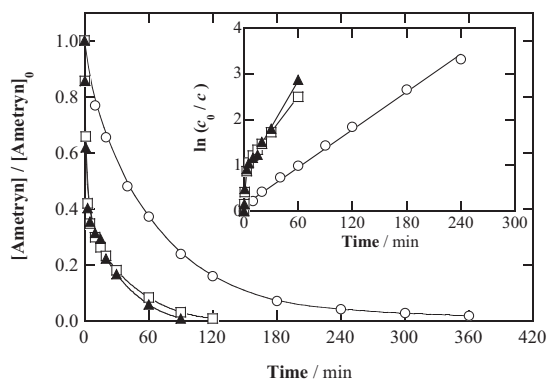


Fig. 5. Variation of the normalized ametryn concentration with electrolysis time for the treatment of 2.5 L of solutions with herbicide formulation of 20 mg L⁻¹ TOC in 0.05 M Na₂SO₄ at pH 3.0 and 35 °C in a flow plant with a BDD/air-diffusion cell at 50 mA cm⁻² and liquid flow rate of 200 L h⁻¹. Method: (○) AO-H₂O₂, (□) EF with 0.50 mM Fe²⁺ and (▲) SPEF with 0.50 mM Fe²⁺. The inset panel presents the corresponding kinetic analysis considering a pseudo-first-order reaction.

Fig. 6a shows that the relative oxidation ability of EAOPs also increases in the sequence AO-H₂O₂ < EF < SPEF. This agrees with the expected slow oxidation of intermediates by BDD(·OH) in AO-H₂O₂, which was upgraded in EF and SPEF by the faster attack of ·OH in the bulk. Note that the acceleration of mineralization in SPEF compared with EF was much smaller for ametryn than for tebuthiuron (see Fig. 2a), which can be explained by the smaller proportion of photosensitive products formed from the former herbicide. After 360 min of electrolysis, TOC was reduced by 24%, 47% and 52% in AO-H₂O₂, EF and SPEF, respectively, values lower than those obtained for tebuthiuron under comparable conditions (see

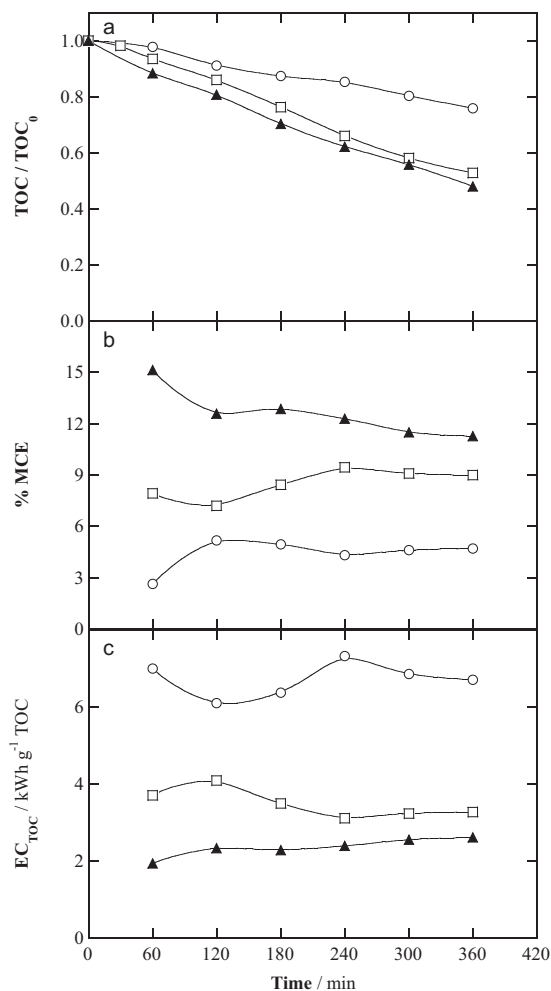


Fig. 6. (a) Normalized TOC removal, (b) mineralization current efficiency and (c) specific energy consumption per unit TOC mass removed for the experiments of Fig. 5. Method: (○) AO-H₂O₂, (□) EF with 0.50 mM Fe²⁺ and (▲) SPEF with 0.50 mM Fe²⁺.

Table 1). The larger persistence of ametryn led to lower current efficiencies and greater EC_{TOC} values, as can be seen in Fig. 6b and c, respectively. At times >120 min, quite constant and increasing MCE values of 4.3–5.1%, 8.4–9.4% and 11.3–12.8% and decreasing EC_{TOC} values of 6.1–6.8, 3.2–3.5 and 2.3–2.6 kWh g⁻¹ TOC were determined in AO-H₂O₂, EF and SPEF, respectively, suggesting a quite constant mineralization rate of intermediates in all cases. Again, the SPEF process required the lowest energy input.

The influence of j between 25 and 100 mA cm⁻² on the EF and SPEF treatments for 0.18 mM ametryn as well as the effect of substrate concentration from 0.04 to 0.72 mM in SPEF at 50 mA cm⁻² were subsequently examined. Fig. SM-1a depicts a slight enhancement of mineralization from 51% to 58% when increasing j for SPEF. A similar behavior was found for the homologous EF treatments (see Table 1). This means that the excess of hydroxyl radicals produced at higher j were primordially consumed by parasitic reactions (12)–(14). This trend was reflected in the progressive fall of MCE for both treatments when j rose. As can be seen in Fig. SM-1b, the current efficiency decayed from 22–26% at 25 mA cm⁻² to 6–7% at 100 mA cm⁻² of SPEF, again indicating that the processes were more efficient at lower j values. Accordingly, Fig. SM-1c evidences that the EC_{TOC} values underwent a gradual growth with raising j , from about 0.85 to 4.5 kWh g⁻¹ TOC when going from 25 to 100 mA cm⁻². The best performance was then obtained at

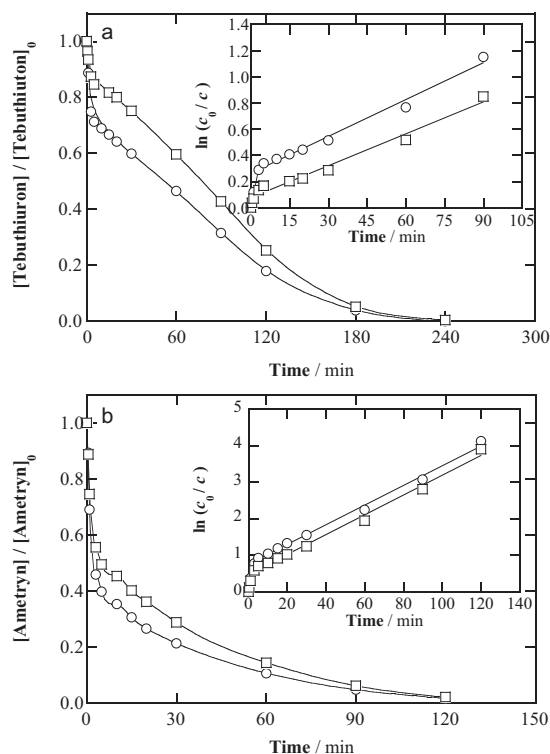


Fig. 7. Normalized concentration abatement of (a) tebuthiuron and (b) ametryn with electrolysis time during the SPEF treatment of 2.5 L of mixtures of herbicide formulations in 0.05 M Na_2SO_4 with 0.50 mM Fe^{2+} at pH 3.0, 35 °C and 50 mA cm^{-2} using a solar flow plant at liquid flow rate of 200 L h^{-1} . Herbicide content: 0.18 mM tebuthiuron with (○) 0.09 mM (1:0.5) and (□) 0.18 mM (1:1) ametryn. The inset panels show the kinetic analysis assuming a pseudo-first-order reaction.

25 mA cm^{-2} , with 51% of mineralization, 21.0% of current efficiency and 0.86 kWh g^{-1} TOC (10.3 kWh m^{-3}) of energy consumption after 360 min of SPEF.

When the effect of increasing substrate content on the performance of the SPEF process was assessed, lower normalized ametryn and TOC removals were found, as in the case of tebuthiuron. Figs. SM-2a and SM-2b show these trends for the ametryn solutions tested. As can be seen, it disappeared at longer times of 30, 90 and 240 min for 0.04, 0.18 and 0.72 mM ametryn, respectively, whereas the percentage of TOC removed at 360 min decreased from 52% for 0.18 mM to 42% for 0.72 mM. An irregular normalized TOC abatement can be observed in Fig. SM-2b at 0.04 mM content, probably by the formation of a larger proportion of recalcitrant products that can be difficultly destroyed by hydroxyl radicals. Fig. SM-2a also shows a quick and decreasing removal of 95%, 60% and 21% of the initial substrate for 0.04, 0.18 and 0.72 mM, respectively, in only 4–5 min of electrolysis. Under these conditions, good linear correlations were obtained up to 0.18 mM considering a pseudo-first-order reaction, as highlights the inset panel of Fig. SM-2a. The corresponding k_1 values at short time given in Table 1 decreased as ametryn concentration grew, being already insignificant for 0.72 mM. For times >5 min, slower pseudo-first-order correlations were obtained and the corresponding lower k_1 values during the second stage, also listed in Table 1, decreased progressively at higher substrate content, as expected by its slower oxidation by similar quantities of $\text{BDD}(\cdot\text{OH})$ and $\cdot\text{OH}$ generated at 50 mA cm^{-2} . This kinetic change can be accounted for by the attack of such radicals onto the easily oxidizable $\text{Fe(II)}\text{-ametryn}$ complexes at short time and the recalcitrant $\text{Fe(III)}\text{-ametryn}$ species at long time, as occurred for tebuthiuron.

Despite the smaller normalized TOC removal with raising ametryn content, greater TOC amount was abated, as a result of the

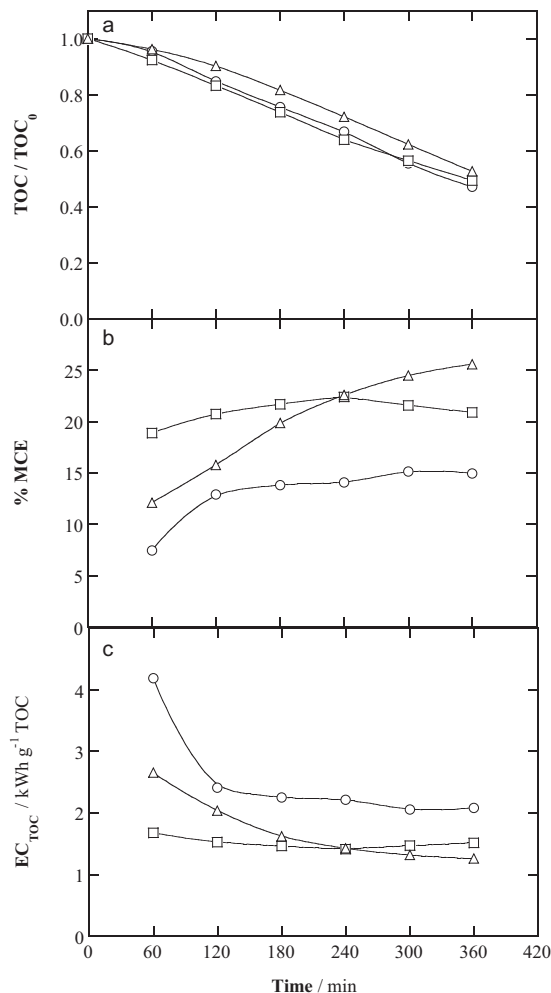


Fig. 8. Change of (a) normalized TOC, (b) mineralization current efficiency and (c) specific energy consumption per unit TOC mass removed with electrolysis time for the degradation of mixtures of herbicide formulations under the same conditions of Fig. 7. Herbicide concentration: 0.18 mM tebuthiuron (20 mg L^{-1} TOC) with (○) 0.09 mM (1:0.5), (□) 0.18 mM (1:1) and (△) 0.36 mM (1:2) ametryn.

gradual deceleration of parasitic reactions (12)–(14), yielding higher MCE and lower EC_{TOC} values (see Table 1). The best performance for this set of trials was then found at the highest concentration tested of 0.72 mM, leading to 42% mineralization with 32.0% of MCE and 1.03 kWh g^{-1} TOC (38.6 kWh m^{-3}) of energy consumption.

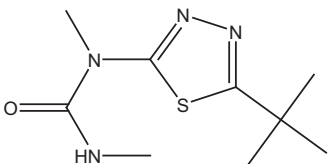
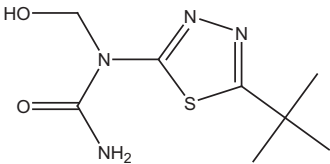
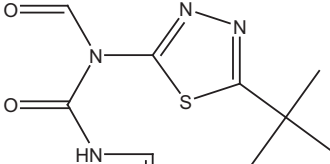
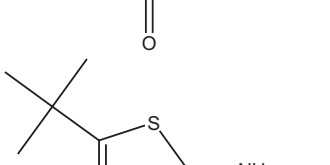
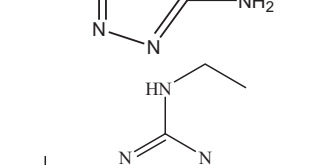
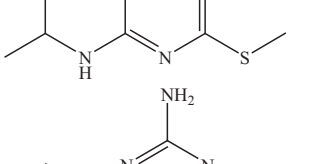
3.3. SPEF degradation of mixed tebuthiuron and ametryn formulations

Mixtures of tebuthiuron and ametryn formulations were degraded by the most powerful EAOP, i.e., SPEF process, to study their mutual influence. The assays were made in the same flow plant upon using 0.18 mM tebuthiuron formulation mixed with 0.09 mM (1:0.5), 0.18 mM (1:1) and 0.36 mM (1:2) ametryn formulation in 0.05 M Na_2SO_4 with 0.50 mM Fe^{2+} at pH 3.0, 35 °C and $j = 50 \text{ mA cm}^{-2}$ for 360 min. No significant pH variation was observed during these trials.

Fig. 7a and b shows the normalized concentration decay of each herbicide for (1:0.5) and (1:1) mixtures. In both cases, tebuthiuron and ametryn were completely removed in about 240 and 120 min, respectively. The lower abatement of the first herbicide was expected from its comparatively slower reaction with $\text{BDD}(\cdot\text{OH})$ and $\cdot\text{OH}$ in single solutions (see Figs. 4a and SM-2a). However,

Table 2

Initial herbicides and their primary heteroaromatic products identified by GC–MS after 180 min of SPEF degradation of 2.5 L of a solution with tebuthiuron (**1a**) and ametryn (**2a**) formulations at equimolar contents of both herbicides in 0.05 M Na₂SO₄ and 0.50 mM Fe²⁺ of pH 3.0 in a solar flow plant with a BDD/air-diffusion cell operating at 50 mA cm^{−2}.

Compound	Molecular structure	Retention time (min)	Ion fragmentation (m/z)
1a		28.4	228 (M ⁺), 171, 156, 88, 74
1b		28.5	230 (M ⁺), 173, 158, 142, 116
1c		28.6	256 (M ⁺), 199, 171, 156
1d		25.2	157 (M ⁺), 142, 100
2a		35.2	227 (M ⁺), 212, 199, 185, 170
2b		32.6	199 (M ⁺), 184, 157, 110

the increase in ametryn content caused a deceleration of the abatement of both herbicides because of the attack of similar amounts of such hydroxyl radicals onto greater organic load. As found for the single formulations at the same concentration, two consecutive pseudo-first-order kinetics related to the removal of their Fe(II) and Fe(III) complexes were found (see the inset panels of Fig. 7a and b). The k_1 values at short and long time for ametryn were 2.6–5.9 times higher than those of tebuthiuron in the mixed solutions and, for the (1:1) mixture, they were much lower than those of the homologous single solutions because of the greater organic load (see Table 1).

Fig. 8a depicts a TOC abatement of 53%, 51% and 48% after 360 min of electrolysis of the (1:0.5), (1:1) and (1:2) mixtures, respectively. The slight loss in oxidation ability with raising ametryn concentration can be associated not only with the presence of more organic load, but also with the fact that the intermediates of this herbicide were more recalcitrant than those of tebuthiuron since similar TOC reductions were found for the mixtures and single ametryn solutions under comparable conditions (see Fig. SM-2a). Fig. 8b shows a rise in the MCE values at greater total organic

content of the mixture, more evident from 240 min of treatment, due to the deceleration of parasitic reactions (12)–(14) by the quicker reaction of BDD(·OH) and ·OH with greater amounts of organic pollutants. This trend was also reflected in the corresponding decay in EC_{TOC} value presented in Fig. 8c. At the end of the treatment of the (1:2) mixture, the highest current efficiency (25.6%) with the lowest EC_{TOC} (1.25 kWh g^{−1} TOC or 36.7 kWh m^{−3}) were achieved (see Table 1a). It is noticeable that the MCE values found for single and mixed formulations of tebuthiuron and ametryn were lower than those obtained for herbicide mecoprop [40] and different azo dyes [41–43] under similar SPEF conditions, which arises from the lower mineralization rate found in this work. This entails higher EC_{TOC} values that make the SPEF process for the present herbicides very expensive from an energy point of view.

The products generated during the first 180 min of treatment of the (1:1) mixture were detected by GC–MS. Table 2 summarizes the molecules found by this technique, including the starting tebuthiuron (**1a**) and ametryn (**2a**) and their identified primary heteroaromatic derivatives. Degradation of **1a** yielded the com-

pound **1b** by hydroxylation and demethylation and the derivative **1c** coming from hydroxylation followed by oxidation to give two aldehyde groups. Moreover, the urea group of **1a** was broken leading to the compound **1d** that contains the remaining amino group linked to the thiadiazole ring. On the other hand, the derivative **2b** corresponding to the deethylation of **2a** was identified as well. The persistence of the heteroaromatic products of **1a** and **2a** explains the partial mineralization achieved for their solutions upon SPEF treatment.

4. Conclusions

The SPEF process with a BDD/air-diffusion cell is able to partially mineralize single tebuthiuron and ametryn formulations. No short-linear carboxylic acids were produced and NO_3^- and SO_4^{2-} ions were released. SPEF was the most viable EAOP and its superiority was due to the additional photo-oxidation of other intermediates and/or their Fe(III) complexes under sunlight irradiation, combined with the oxidation by hydroxyl radicals. For herbicide concentrations up to 0.18 mM, a two-stage pseudo-first-order kinetics was found in EF and SPEF. The initial kinetics was very rapid, appeared at short time and was ascribed to the abatement of the Fe(II) complexes of the herbicides. It was followed by a much slower kinetics associated with the decay of their Fe(III) complexes. Ametryn disappeared more quickly than tebuthiuron, whereas its solutions were more slowly mineralized. Higher j accelerated the abatement of herbicides and the mineralization process, but with lower MCE and greater EC_{TOC} values. The opposite trend was found when increasing herbicide content. Mixtures of both formulations treated by SPEF showed a drop in the removal rate of herbicides compared to that of single solutions at the same concentration, along with a loss in mineralization ability that became similar to that of the recalcitrant solutions of the single ametryn formulation. Four primary heteroaromatics were identified at long electrolysis time of an equimolar mixture, being their large persistence the key to explain the partial mineralization achieved in SPEF. Under comparable conditions, SPEF was much more powerful than $\text{AO-H}_2\text{O}_2$ for the remediation of wastewater polluted with single and mixed herbicides, because it yielded quicker substrate decay and greater mineralization, ending in higher current efficiency and lower EC_{TOC} , which demonstrates the positive synergistic effect of hydroxyl radicals and sunlight to remove organic products generated from tebuthiuron and ametryn.

Acknowledgments

Financial support from project CTQ2013-48897-C2-1-R from MINECO (Spain), co-financed with FEDER funds, as well as from FUNDECT, CAPES and CNPq (Brazil), is acknowledged.

Appendix A. Supplementary data

Supplementary data associated with this article can be found, in the online version, at <http://dx.doi.org/10.1016/j.cej.2016.02.026>.

References

- [1] S. Chiron, A.R. Fernandez-Alba, A. Rodriguez, E. Garcia-Calvo, Pesticide chemical oxidation: state-of-the-art, *Water Res.* 34 (2000) 366–377.
- [2] M.R.A. Silva, A.G. Trovó, R.F.P. Nogueira, Degradation of the herbicide tebuthiuron using solar photo-Fenton process and ferric citrate complex at circumneutral pH, *J. Photochem. Photobiol. A: Chem.* 191 (2007) 187–192.
- [3] C. Lourencetti, M.R. Rodrigues de Marchi, M.L. Ribeiro, Determination of sugar cane herbicides in soil and soil treated with sugar cane vinasse by solid-phase extraction and HPLC-UV, *Talanta* 77 (2008) 701–709.
- [4] V.L. Ferracini, S.C.N. Queiroz, M.A.F. Santos, G.L. Gomes, Method for determination of hexazinone and tebuthiuron in water, *Quim. Nova* 28 (2005) 380–382.
- [5] L. Diaz, J. Llorca-Porcel, I. Valor, Ultra trace determination of 31 pesticides in water samples by direct injection-rapid resolution liquid chromatography-electrospray tandem mass spectrometry, *Anal. Chim. Acta* 624 (2008) 90–96.
- [6] M. Muneer, M. Qamar, M. Saquib, D.W. Bahnemann, Heterogeneous photocatalysed reaction of three selected pesticide derivatives, protham, propachlor and tebuthiuron in aqueous suspensions of titanium dioxide, *Chemosphere* 61 (2005) 457–468.
- [7] W. Bahnemann, M. Muneer, M.M. Haque, Titanium dioxide-mediated photocatalysed degradation of few selected organic pollutants in aqueous suspensions, *Catal. Today* 124 (2007) 133–148.
- [8] R.F.P. Nogueira, M.R.A. Silva, A.G. Trovó, Influence of the iron source on the solar photo-Fenton degradation of different classes of organic compounds, *Sol. Energy* 79 (2005) 384–392.
- [9] M.R.A. Silva, W. Vilegas, M.V.B. Zanoni, R.F.P. Nogueira, Photo-Fenton degradation of the herbicide tebuthiuron under solar irradiation: iron complexation and initial intermediates, *Water Res.* 44 (2010) 3745–3753.
- [10] I. Sirés, E. Brillas, Remediation of water pollution caused by pharmaceutical residues based on electrochemical separation and degradation technologies: a review, *Environ. Int.* 40 (2012) 212–229.
- [11] B. Xu, N.-Y. Gao, H. Cheng, C.-Y. Hu, S.-J. Xia, X.-F. Sun, X. Wang, S. Yang, Ametryn degradation by aqueous chlorine: kinetics and reaction influences, *J. Hazard. Mater.* 169 (2009) 586–592.
- [12] N.-Y. Gao, Y. Deng, D. Zhao, Ametryn degradation in the ultraviolet (UV) irradiation/hydrogen peroxide (H_2O_2) treatment, *J. Hazard. Mater.* 164 (2009) 640–645.
- [13] S.L.H. Rebelo, A. Melo, R. Coimbra, M.E. Azenha, M.M. Pereira, H.D. Burrows, M. Sarakha, Photodegradation of atrazine and ametryn with visible light using water soluble porphyrins as sensitizers, *Environ. Chem. Lett.* 5 (2007) 29–33.
- [14] J.C. Márquez, F.M. Martínez, G. Li Puma, Photocatalytic mineralization of commercial herbicides in a pilot-scale solar CPC reactor: photoreactor modeling and reaction kinetics constants independent of radiation field, *Environ. Sci. Technol.* 43 (2009) 8953–8960.
- [15] S.A. Alves, T.C.R. Ferreira, N.S. Sabatini, A.C.A. Trientini, F.L. Migliorini, M.R. Baldan, N.G. Ferreira, M.R.V. Lanza, A comparative study of the electrochemical oxidation of the herbicide tebuthiuron using boron-doped diamond electrodes, *Chemosphere* 88 (2012) 155–160.
- [16] M. Panizza, G. Cerisola, Direct and mediated anodic oxidation of organic pollutants, *Chem. Rev.* 109 (2009) 6541–6569.
- [17] I. Sirés, E. Brillas, M.A. Oturan, M.A. Rodrigo, M. Panizza, Electrochemical advanced oxidation processes: today and tomorrow. A review, *Environ. Sci. Pollut. Res.* 21 (2014) 8336–8367.
- [18] S. Vasudevan, M.A. Oturan, Electrochemistry: as cause and cure in water pollution—an overview, *Environ. Chem. Lett.* 12 (2014) 97–108.
- [19] M. Hamza, R. Abdelhedi, E. Brillas, I. Sirés, Comparative electrochemical degradation of the triphenylmethane dye Methyl Violet with boron-doped diamond and Pt anodes, *J. Electroanal. Chem.* 627 (2009) 41–50.
- [20] L. Ciriaco, C. Anjo, J. Correia, M.J. Pacheco, A. Lopes, Electrochemical degradation of ibuprofen on Ti/Pt/PbO₂ and Si/BDD electrodes, *Electrochim. Acta* 54 (2009) 1464–1472.
- [21] M.A. Rodrigo, P. Cañizares, A. Sánchez-Carretero, C. Sáez, Use of conductive-diamond electrochemical oxidation for wastewater treatment, *Catal. Today* 151 (2010) 173–177.
- [22] E.B. Cavalcanti, S. Garcia-Segura, F. Centellas, E. Brillas, Electrochemical incineration of omeprazole in neutral aqueous medium using a platinum or boron-doped diamond. Degradation kinetics and oxidation products, *Water Res.* 47 (2013) 1803–1815.
- [23] A. Thiam, I. Sirés, J.A. Garrido, R.M. Rodríguez, E. Brillas, Decolorization and mineralization of Allura Red AC aqueous solutions by electrochemical advanced oxidation processes, *J. Hazard. Mater.* 290 (2015) 34–42.
- [24] B. Boye, P.A. Michaud, B. Marselli, M.M. Dieng, E. Brillas, C. Comninellis, Anodic oxidation of 4-chlorophenoxyacetic acid on synthetic boron-doped diamond electrodes, *New Diamond Front. Carbon Technol.* 12 (2002) 63–72.
- [25] B. Marselli, J. Garcia-Gomez, P.A. Michaud, M.A. Rodrigo, C. Comninellis, Electrogeneration of hydroxyl radicals on boron-doped diamond electrodes, *J. Electrochem. Soc.* 150 (2003) D79–D83.
- [26] E. Guinea, E. Brillas, F. Centellas, P. Cañizares, M.A. Rodrigo, C. Saez, Oxidation of enrofloxacin with conductive-diamond electrochemical oxidation, ozonation and Fenton oxidation, a comparison, *Water Res.* 43 (2009) 2131–2138.
- [27] M.H.M.T. Assumpção, A. Moraes, R.F.B. De Souza, R.M. Reis, R.S. Rocha, I. Gaubeur, M.L. Calegario, P. Hammer, M.R.V. Lanza, M.C. Santos, Degradation of dipyrone via advanced oxidation processes using a cerium nanostructured electrocatalyst material, *Appl. Catal. A: Gen.* 462–463 (2013) 256–261.
- [28] A. Wang, J. Qu, H. Liu, J. Ru, Mineralization of an azo dye Acid Red 14 by photoelectro-Fenton process using an activated carbon fiber cathode, *Appl. Catal. B: Environ.* 84 (2008) 393–399.
- [29] A. Khataee, A. Akbarpour, B. Vahi, Photoassisted electrochemical degradation of an azo dye using Ti/RuO₂ anode and carbon nanotubes containing gas-diffusion cathode, *J. Taiwan Inst. Chem. Eng.* 45 (2014) 930–936.
- [30] V. Vatanpour, N. Daneshvar, M.H. Rasoulifard, Electro-Fenton degradation of synthetic dye mixture: influence of intermediates, *J. Environ. Eng. Manage.* 19 (2009) 277–282.

- [31] M.A. Oturan, M.C. Edelahai, N. Oturan, K. El Kacemi, J.J. Aaron, Kinetics of oxidative degradation/mineralization pathways of the phenylurea herbicides diuron, monuron and fenuron in water during application of the electro-Fenton process, *Appl. Catal. B: Environ.* 97 (2010) 82–89.
- [32] A. Dirany, I. Sirés, N. Oturan, A. Özcan, M.A. Oturan, Electrochemical treatment of the antibiotic sulfachloropyridazine: kinetics, reaction pathways, and toxicity evolution, *Environ. Sci. Technol.* 46 (2012) 4074–4082.
- [33] A. El-Ghenmy, R.M. Rodríguez, E. Brillas, N. Oturan, M.A. Oturan, Electro-Fenton degradation of the antibiotic sulfanilamide with Pt/carbon-felt and BDD/carbon-felt cells. Kinetics, reaction intermediates, and toxicity assessment, *Environ. Sci. Pollut. Res.* 21 (2014) 8368–8378.
- [34] N. Borràs, R. Oliver, C. Arias, E. Brillas, Degradation of atrazine by electrochemical advanced oxidation processes using a boron-doped diamond anode, *J. Phys. Chem. A* 114 (2010) 6613–6621.
- [35] A.R.F. Pipi, I. Sirés, A.R. De Andrade, E. Brillas, Application of electrochemical advanced oxidation processes to the mineralization of the herbicide diuron, *Chemosphere* 109 (2014) 49–55.
- [36] A. Thiam, M. Zhou, E. Brillas, I. Sirés, Two-step mineralization of Tartrazine solutions: study of parameters and by-products during the coupling of electrocoagulation with electrochemical advanced oxidation processes, *Appl. Catal. B: Environ.* 150–151 (2014) 116–125.
- [37] K. Cruz-González, O. Torres-López, A. García-León, E. Brillas, A. Hernández-Ramírez, J.M. Peralta-Hernández, Optimization of electro-Fenton/BDD process for decolorization of a model azo dye wastewater by means of response surface methodology, *Desalination* 286 (2012) 63–68.
- [38] E. Brillas, I. Sirés, M.A. Oturan, Electro-Fenton process and related electrochemical technologies based on Fenton's reaction chemistry, *Chem. Rev.* 109 (2009) 6570–6631.
- [39] M.A. Oturan, J.J. Aaron, Advanced oxidation processes in water/wastewater treatment: principles and applications. A review, *Crit. Rev. Environ. Sci. Technol.* 44 (2014) 2577–2641.
- [40] C. Flox, J.A. Garrido, R.M. Rodríguez, P.L. Cabot, F. Centellas, C. Arias, E. Brillas, Mineralization of herbicide mecoprop by photoelectro-Fenton with UVA and solar light, *Catal. Today* 129 (2007) 29–36.
- [41] E.J. Ruiz, A. Hernández-Ramírez, J.M. Peralta-Hernández, C. Arias, E. Brillas, Application of solar photoelectro-Fenton technology to azo dyes mineralization: effect of current density, Fe^{2+} and dye concentration, *Chem. Eng. J.* 171 (2011) 385–392.
- [42] F.C. Moreira, S. García-Segura, V.J.P. Vilar, R.A.R. Boaventura, E. Brillas, Decolorization and mineralization of Sunset Yellow FCF azo dye by anodic oxidation, electro-Fenton, UVA photoelectro-Fenton and solar photoelectro-Fenton processes, *Appl. Catal. B: Environ.* 142–143 (2013) 877–890.
- [43] A. Thiam, I. Sirés, F. Centellas, P.L. Cabot, E. Brillas, Decolorization and mineralization of Allura Red AC azo dye by solar photoelectro-Fenton: identification of intermediates, *Chemosphere* 136 (2015) 1–8.